

Decoding the metabolic landscape of pathophysiological stress-induced cell death in anucleate red blood cells

Travis Nemkov¹, Syed M. Qadri^{2,3,4}, William P. Sheffield^{3,4}, Angelo D'Alessandro¹



¹Department of Biochemistry and Molecular Genetics, University of Colorado Denver - Anschutz Medical Campus, Aurora, CO, USA; ²Faculty of Health Sciences, Ontario Tech University, Oshawa, ON, Canada; ³Centre for Innovation, Canadian Blood Services, Hamilton, ON, Canada; ⁴Department of Pathology and Molecular Medicine, McMaster University, Hamilton, ON, Canada

Background - In response to stress, anucleate red blood cells (RBCs) can undergo a process of atypical cell death characterised by intracellular Ca²⁺ accumulation and phosphatidylserine (PS) externalisation. Here we studied alterations in RBC metabolism, a critical contributor to their capacity to survive environmental challenges, during this process.

Materials and methods - Metabolomics analyses of RBCs and supernatants, using ultra-high-pressure liquid chromatography coupled to mass spectrometry, were performed after *in vitro* exposure of RBCs to different pathophysiological cell stressors, including starvation, extracellular hypertonicity, hyperthermia, and supraphysiological ionic stress. Cell death was examined by flow cytometry.

Results - Our data show that artificially enhancing RBC cytosolic Ca²⁺ influx significantly enhanced purine oxidation and strongly affected cellular bioenergetics by reducing glycolysis. Depleting extracellular Ca²⁺ curtailed starvation-induced cell death, an effect paralleled by the activation of compensatory pathways such as the pentose phosphate pathway, carboxylic acid metabolism, increased pyruvate to lactate ratios (methemoglobin reductase activation), one-carbon metabolism (protein-damage repair) and glutathione synthesis; RBCs exposed to hypertonic shock displayed a similar metabolic profile. Furthermore, cell stress promoted lipid remodelling as reflected by the levels of free fatty acids, acyl-carnitines and CoA precursors. Notably, RBC PS exposure, independently of the stressor, showed significant correlation with the levels of free fatty acids, glutamate, cystine, spermidine, tryptophan, 5-oxoproline, lactate, and hypoxanthine.

Discussion - In conclusion, different cell death-inducing pathophysiological stressors, encountered in various clinical conditions, result in differential RBC metabolic phenotypes, only partly explained by intracellular Ca²⁺ levels and ATP availability.

Keywords: calcium, cell death, metabolomics, pathophysiological stress, red blood cells.

INTRODUCTION

Under physiological conditions, circulating red blood cells (RBCs) have an average lifespan of approximately 100-120 days, a time window during which they progressively become senescent prior to removal from circulation *via* erythrophagocytosis through the reticuloendothelial system in the liver and spleen^{1,2}. However, following acute

Arrived: 21 October 2019
Revision accepted: 28 November 2019
Correspondence: Angelo D'Alessandro
e-mail: angelo.dalessandro@cuanschutz.edu

insults, anucleate RBCs are prematurely cleared from the circulation through an atypical cell death process, also referred to as eryptosis³⁻⁶. Injured RBCs progressing to cell death display a plethora of morphological changes, including a disruption in their membrane phospholipid asymmetry causing phosphatidylserine (PS) externalisation⁴. Given that the loss of phospholipid asymmetry in RBCs, and other cell types, is mediated by the activity of ATP-dependent enzymes⁷, PS externalisation, thus, offers a window into the cellular metabolic state. Physiologically, swift RBC clearance by cell death is believed to avert extracellular haemoglobin accumulation in blood vessels by diverting them to splenic catabolism¹. Red blood cell lifespan in the circulation is influenced by age-related alterations⁸, and may also be impacted by pathophysiological cell stressors such as extracellular hypertonicity, hyperthermia, and energy starvation, encountered in a wide array of clinical conditions^{3,4}. These cell stressors elicit supraphysiological intracellular Ca^{2+} levels by increased membrane cation conductance, which, in turn, influence various components of the cytoskeleton and modulate multiple signalling cascades involving Ca^{2+} -sensitive enzymes leading to cellular dysfunction and death^{2,4}. Mechanistically, however, these pathophysiological cell stressors may also differentially activate various non- Ca^{2+} -dependent pathways (reviewed by Lang *et al.*³ and Qadri *et al.*⁴). The ionic stress due to supraphysiological Ca^{2+} overload, caused by cell stress, may be pharmacologically recapitulated using Ca^{2+} ionophores⁹. While ionic homeostasis in RBCs is, at least in part, energy- and temperature-dependent¹⁰⁻¹², the patterns of metabolic reprogramming under stress-mediated cytoplasmic Ca^{2+} increase remain elusive. From a metabolic standpoint, the case of RBCs is particularly striking in that the absence of mitochondria has prompted investigators to focus mainly on cytosolic reactions such as glycolysis, pentose phosphate pathway, and Rapoport-Luebering shunt¹². In the last decade, however, several unexpected biochemical pathways in mitochondria-devoid RBCs have been discovered with the advent of high-throughput metabolomic approaches in the ageing RBC *in vivo*¹³ and *in vitro*, i.e., under blood bank conditions^{14,15}. There is increasing evidence to support the notion that metabolic changes regulate cell-fate decisions¹⁶⁻¹⁸. In nucleated cells, growth factors

enable metabolic checkpoints to promote proliferation and apoptosis¹⁶. Similar considerations hold true for RBCs, since the energy-deficient effete RBCs are rapidly removed from the bloodstream due to impaired membrane deformability¹⁹. The role of mitochondria in the metabolism and intrinsic apoptosis cascade of nucleated cells is well established²⁰. In mitochondria-devoid RBCs, however, the current understanding into the metabolic alterations during their extracellular environment changes and cell death remains rudimentary. The present study, thus, aimed to dissect the intracellular and extracellular metabolome of injury-afflicted RBCs undergoing atypical cell death, by examining RBCs lysates and supernatants, respectively.

MATERIALS AND METHODS

Red blood cell treatment and flow cytometry analysis

Red blood cell component production from five healthy consenting donors was performed by the Canadian Blood Services (CBS) Network Centre for Applied Development (netCAD, Vancouver, BC, Canada; approved by CBS Research Ethics Board #2015.022). The log₄ leukocyte-filtered RBC concentrates were shipped to McMaster University, Hamilton, ON, Canada, under refrigerated conditions. RBCs (10% haematocrit) were exposed to different pathophysiological conditions by incubation in different solutions at specified temperatures and time durations. To study the impact of starvation on RBC metabolism and cell death, RBCs were incubated at 37 °C for 48 hours (h) in Ringer's solution (containing 125 mM NaCl, 5 mM KCl, 5 mM glucose, 32 mM HEPES, 1 mM Mg_2SO_4 , 1 mM CaCl_2 ; pH 7.4) or in a modified Ringer's solution with omission of either glucose alone or both glucose and CaCl_2 . Where indicated, RBCs were exposed to increased extracellular osmolality by incubation in hypertonic Ringer's solution containing sucrose (550 mM) for 6 h. Elevation in intracellular Ca^{2+} was stimulated by treatment of RBCs with the Ca^{2+} ionophore ionomycin (10 μM for 1 h at 37 °C; Sigma, St. Louis, MO, USA). To examine metabolic alterations in temperature-sensitive cell death, RBCs were incubated in Ringer's solution for 12 h at 37 °C (normothermia) or 40 °C (hyperthermia). Baseline measurements were performed in RBCs drawn directly from blood bags stored (<5 days) under blood bank conditions. At the end of the respective treatment,

RBC samples were centrifuged (272 *g* at 4 °C for 5 min) and the RBC pellet and the respective supernatants were transferred in separate cryotubes and snap frozen in liquid nitrogen. A small aliquot of RBCs from the treated samples was used to examine cellular markers of cell death using FACS analysis. Fluorescence intensity was determined in the FL1 channel with an excitation wavelength of 488 nm and an emission wavelength of 530 nm using EPICS XL-MCL (Beckman Coulter, Mississauga, ON, Canada) flow cytometer as described previously²¹. To quantify the percentage of PS externalisation, RBCs were stained with annexin V-FITC (1:200; ImmunoTools, Friesoythe, Germany) in Ringer's solution containing an additional 4 mM CaCl₂ for 15 minutes (min) at 37 °C. For the determination of intracellular Ca²⁺ levels, RBCs were loaded with Fluo3/AM (2 μM in Ringer's solution; EMD Millipore Corp., Billerica, MA, USA) for 15 min at 37 °C. All data generated using FACS analysis were analysed using FlowJo® software (FlowJo LLC, Ashland, OR, USA). Frozen RBC samples were shipped on dry ice for metabolomics analyses to the University of Colorado, Aurora, CO, USA.

Sample preparation

Prior to LC-MS analysis, RBCs and supernatant isolates were placed on ice and diluted 1:10 (v/v) or 1:25 (v/v) with methanol:acetonitrile:water (5:3:2, v:v), respectively. Suspensions were vortexed continuously for 30 min at 4 °C. Insoluble material was removed by centrifugation at 10,000 *g* for 10 min at 4 °C and supernatants were isolated for metabolomics analysis by ultra-high performance liquid chromatography-tandem mass spectrometry (UHPLC-MS).

Ultra-high performance liquid chromatography-tandem mass spectrometry analysis

Analyses were performed as previously described^{22,23}. Briefly, the analytical platform employs a Vanquish UHPLC system (Thermo Fisher Scientific, San Jose, CA, USA) coupled online to a Q Exactive mass spectrometer (Thermo Fisher Scientific, San Jose, CA, USA). Samples were resolved over a Kinetex C18 column, 2.1×150 mm, 1.7 μm particle size (Phenomenex, Torrance, CA, USA) equipped with a guard column (SecurityGuard™ Ultracartridge - UHPLC C18 for 2.1 mm ID Columns - AJO-8782 - Phenomenex, Torrance, CA, USA) using an aqueous phase (A) of water and 0.1% formic acid and a mobile phase (B) of acetonitrile and 0.1% formic acid.

Samples were eluted from the column using either an isocratic elution of 5% B flowed at 250 μL/min and 25°C or a gradient from 0-5% B over 0.5 min; 5-95% B over 0.6 min, hold at 95% B for 1.65 min; 95-5% B over 0.25 min; hold at 5% B for 2 min, flowed at 450 μL min⁻¹ and 35°C. The Q Exactive mass spectrometer (Thermo Fisher Scientific, San Jose, CA, USA) was operated independently in positive or negative ion mode, scanning in Full MS mode (2 μscans) from 60 to 900 m z⁻¹ at 70,000 resolution, with 4 kV spray voltage, 45 sheath gas, 15 auxiliary gas. Calibration was performed prior to analysis using the Pierce™ Positive and Negative Ion Calibration Solutions (Thermo Fisher Scientific). Acquired data were then converted from .raw to .mzXML file format using Mass Matrix (Cleveland, OH, USA). Samples were analysed in randomised order with a technical mixture injected after every 15 samples to qualify instrument performance. Metabolite assignments, isotopologue distributions, and correction for expected natural abundances of deuterium, ¹³C, and ¹⁵N isotopes were performed using MAVEN (Princeton, NJ, USA)²⁴.

Graphs, heat maps and statistical analyses (either *t*-test or ANOVA), metabolic pathway analysis, partial least square-discriminant analyses (PLS-DA) and hierarchical clustering was performed using the MetaboAnalyst 3.0 package (www.metaboanalyst.com). Hierarchical clustering analysis (HCA) was also performed through the software GENE-E (Broad Institute, Cambridge, MA, USA). XY graphs were plotted through GraphPad Prism 5.0 (GraphPad Software Inc., La Jolla, CA, USA).

RESULTS

Metabolic effects of red blood cell death-inducing stressors

In the present study, we investigated the metabolic impact of starvation, hyperosmolarity, ionic or temperature stress on human RBCs (n=5) and their respective supernatants (**Figure 1A**). All the raw measurements are provided in *Online Supplementary Content, Tables SI and SII* for RBCs and supernatants, respectively. Multivariate analyses were performed, including hierarchical clustering analyses (HCA) and PLS-DA. A vectorial version of the HCAs for RBCs and supernatants is provided in *Online Supplementary Content, Figures S1 and S2*. Significant metabolic changes by ANOVA are highlighted in **Figure 1B, C and F** for RBCs and supernatants, respectively. These changes indicate

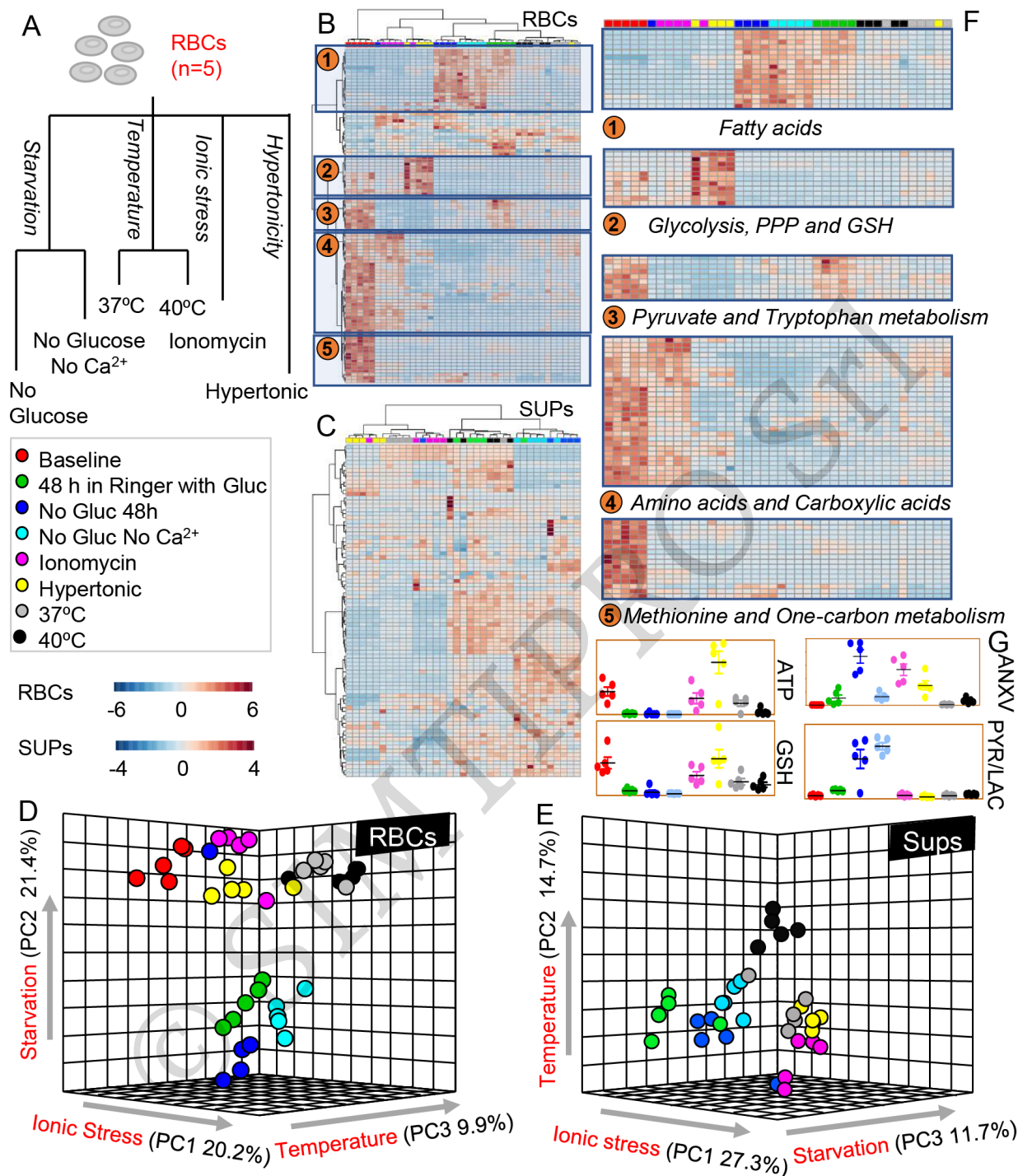


Figure 1 - Metabolomics profiling of cell death-inducing stresses in red blood cells (RBCs) and supernatants. Overview of the experimental design. Briefly, RBCs were either tested at baseline (red) or incubated for 48 hours (h) in Ringer's solution (green). RBCs were either stressed by starvation, i.e., without glucose (dark blue), without glucose and Ca²⁺ (light blue) or ionic stress, i.e., incubation in presence of ionomycin (violet) or under hypertonic conditions (yellow). RBCs were independently incubated for 12 h at 37°C (grey) or 40°C (black) to test the impact of temperature on RBC metabolism. (B and C) and (D and E) Heat maps with hierarchical clustering of the top 50 significant metabolites by ANOVA and partial least square-discriminant analyses (PLS-DA) are shown for RBCs and supernatants, respectively. (F) Top metabolic pathways impacted by the various stresses are highlighted. (G) RBC key metabolites are highlighted, colour-coded as per the legend on the left-hand side of the figure. ANXV: Annexin V binding; ATP: adenosine triphosphate; Gluc: glucose; GSH: glutathione; PPP: pentose phosphate pathway; PYR/LAC: pyruvate to lactate ratio.

a significant metabolic heterogeneity across RBCs treated with different stressors, as further highlighted by PLS-DAs in **Figure 1D** and **E**. In particular, ionic stress with ionomycin resulted in the most severe metabolic changes across all treatments (Principal Component [PC1] accounting for 20-27% of total variance in RBCs and supernatants, respectively), closely followed by starvation (21% variance in RBCs and 11.7% in supernatants), and temperature (9.9% in RBCs and 14.7% in supernatants) (**Figure 1D** and **E**). Pathway analyses suggested a significant impact of starvation on lipid remodelling and free fatty acids, while hypertonic stress significantly impacted glycolysis, the pentose phosphate pathway (PPP) and glutathione metabolism (**Figure 1F**). Ionomycin treatment, but not hyperosmotic stress or starvation without Ca^{2+} , resulted in the intracellular accumulation of amino acids and carboxylic acids in comparison to other stressors (**Figure 1F**). Indeed, hyperosmotic stress, with addition of sucrose, promoted energy metabolism (ATP generation and glutathione levels) above baseline values (**Figure 1G**). On the other hand, starvation promoted significant increases in pyruvate to lactate ratios, suggestive of impaired homeostasis of reducing equivalents (**Figure 1G**). Measurements of annexin V binding indicate that glucose starvation (but not glucose starvation in absence of Ca^{2+}) and ionomycin treatment induced the highest elevation in PS exposure in the outer membrane leaflet (**Figure 1G**).

Metabolic impact of glucose starvation in the presence or absence of extracellular calcium

After a preliminary overview of the data, we then focused on the metabolic impact of glucose starvation on the metabolomes of RBCs and supernatants. Results indicate a significant impact of glucose starvation, accounting for 26-30% of the total metabolic variance in the PLS-DAs of treated RBCs and supernatants, respectively (**Figure 2A** and **C**). HCA of the top 25 significant metabolites in RBCs and supernatants (**Figure 2B** and **D**, respectively) indicate a significant impact of glucose starvation on glycolysis, resulting in significant decreases in glucose, glycolytic intermediates and lactate. These changes were accompanied by significant decreases in total levels of glutathione and increases in the levels of its precursors, glutamate, cysteine and gamma-glutamyl-intermediates, suggestive of dysregulation in (ATP-dependent) glutathione synthesis and turn-over (**Figure 2B**, centre

panel). However, glucose starvation in the absence of Ca^{2+} , though insufficient to rescue the deficit in ATP generation, resulted in a compensatory activation of the PPP (6-phosphogluconate, ribose phosphate). Notably, supernatant levels of acetylcholine and polyamines (spermidine) increased response to glucose starvation and even more so after glucose starvation in the absence of Ca^{2+} . Significant decreases in the levels of free amino acids and carboxylic acids were noted, suggestive of a disruption of amino acid uptake/release and alteration of the enzymatic activity of cytosolic isoforms of Krebs cycle enzymes involved in the metabolism of reducing equivalents (e.g., NADH, NADPH) and salvage reactions¹⁴. Notably, increased intracellular Ca^{2+} levels and PS exposure induced by glucose starvation were normalised back to control levels when RBCs were glucose-starved in calcium-free media (**Figure 2**, centre panel, number 1 and 2 highlights).

Metabolic impact of ionic and hypertonic stress

Partial least square-discriminant analyses revealed a strong impact of ionomycin (38% of the variance [PC1]) on the metabolomes of RBCs (**Figure 3A**). Hypertonicity had a significant impact on RBC metabolism, only partially overlapping with ionomycin. Hyperosmolality increased RBC levels of glutathione and ATP, while ionomycin promoted purine deamination and accumulation of oxidation products of deaminate purines, including hypoxanthine and xanthine (**Figure 3B-D**). Ionomycin promoted alterations to amino acid metabolism (higher levels of free amino acids and carboxylic acids in comparison to hyperosmolality (*Online Supplementary Content*, **Figures S1** and **S2**). Consistent with the metabolomics finding suggesting higher stress in ionomycin-treated cells, intracellular Ca^{2+} levels and PS exposure were significantly higher in ionomycin-treated RBCs as compared to RBCs exposed to hypertonic media (**Figure 3**, centre panel, number 1 and 2 highlights).

Metabolic impact of heat stress

Incubation at 40 °C vs 37 °C significantly impacted RBC metabolism (approx. 22% of total variance), with some subjects responding with extreme metabolic aberrations (PC2 in **Figure 4A** and **C**) and PS exposure above three times the standard deviation of the group average (**Figure 4**, centre panel, number 2 highlight). Heat stress was accompanied by intracellular Ca^{2+} accumulation, increased purine

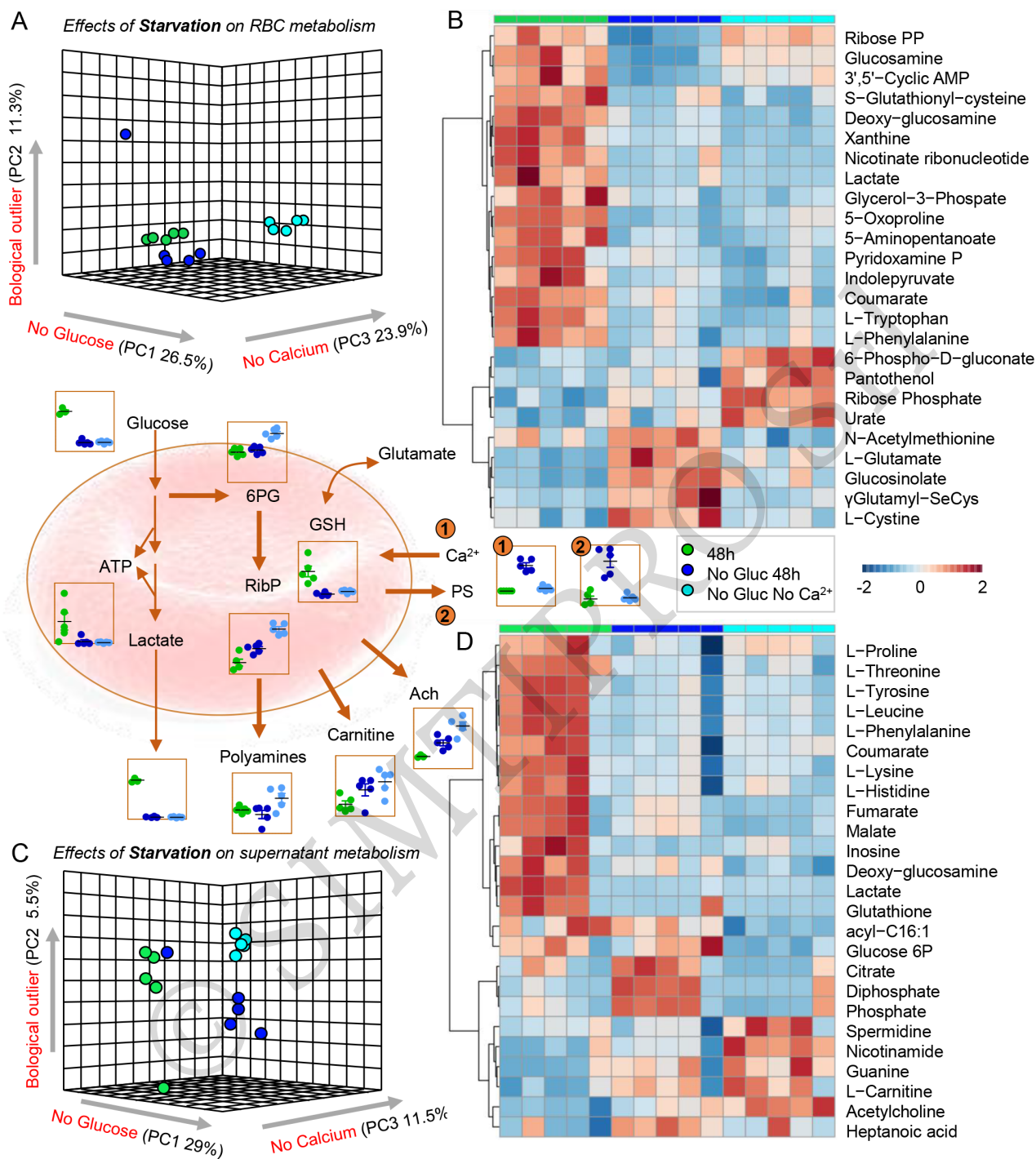


Figure 2 - Metabolic impact of energy starvation.

(A and C) Partial least square-discriminant analyses (PLS-DA) reveals significant impact of both glucose starvation and glucose starvation in the absence of Ca²⁺ in red blood cells (RBCs) and supernatants, respectively. (B and D) Top 25 significant metabolites following starvation stress by ANOVA in RBCs and supernatants, respectively. Key metabolites are highlighted in the dot plots in the centre of the figure, colour-coded as per the legend on the right-hand side of the figure. Ach: acetylcholine; ATP: adenosine triphosphate; GSH: glutathione; PS: phosphatidylserine; RibP: ribose phosphate; 6PG: 6-phosphogluconolactone.

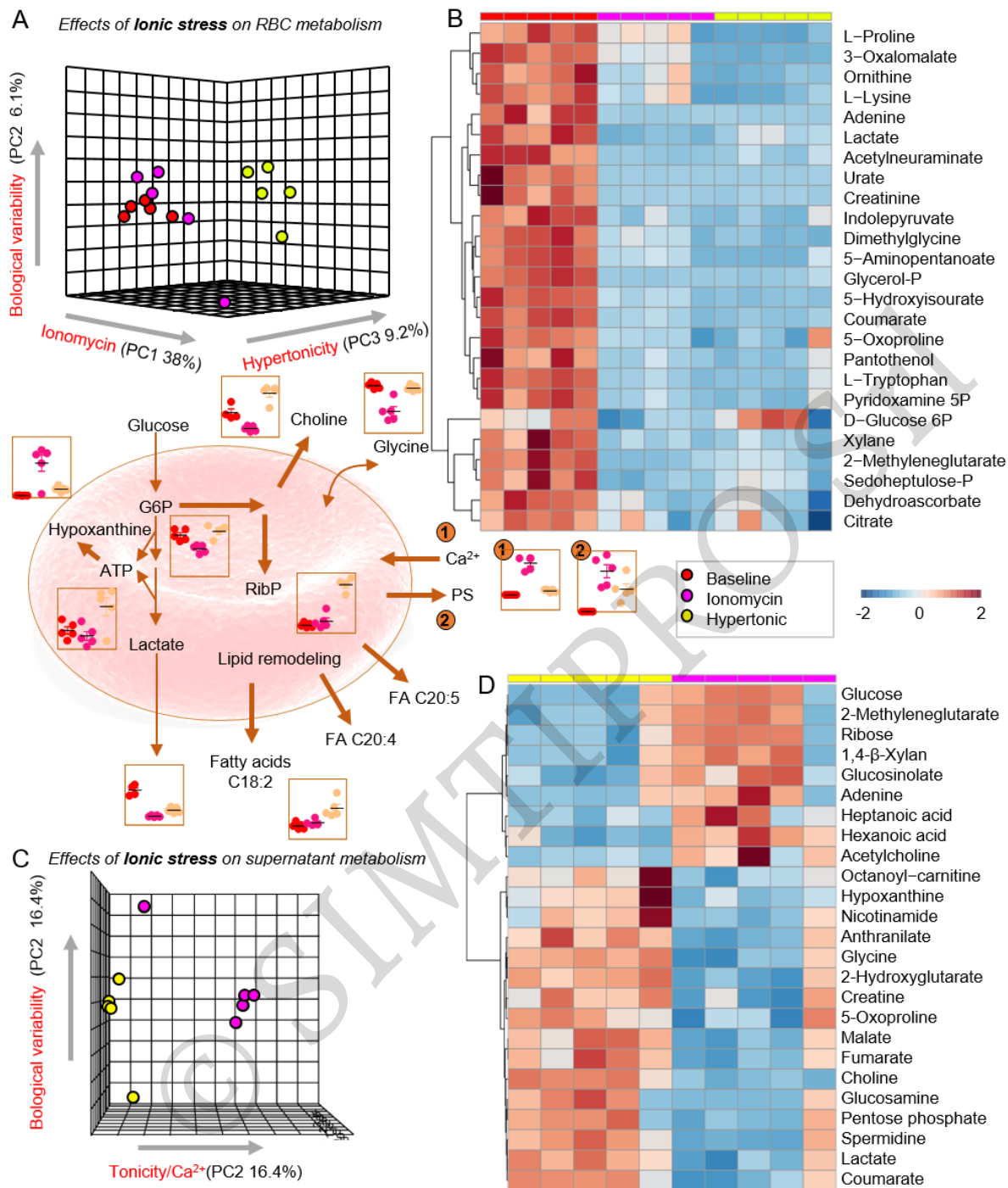


Figure 3 - Metabolic impact of supraphysiological ionic and hypertonic stress.

(A and C) Partial least square-discriminant analyses (PLS-DA) reveals significant impact of ionic stress (which induces increases in intracellular Ca^{2+}) or hypertonic stress in red blood cells (RBCs) and supernatants, respectively. (B and D) Top 25 significant metabolites by ANOVA in RBCs and supernatants are shown. Key metabolites are highlighted in the dot plots in the centre of the figure, colour-coded as per the legend on the right-hand side of the figure.

ATP: adenosine triphosphate; G6P: glucose 6-phosphate; PS: phosphatidylserine; RibP: ribose phosphate.

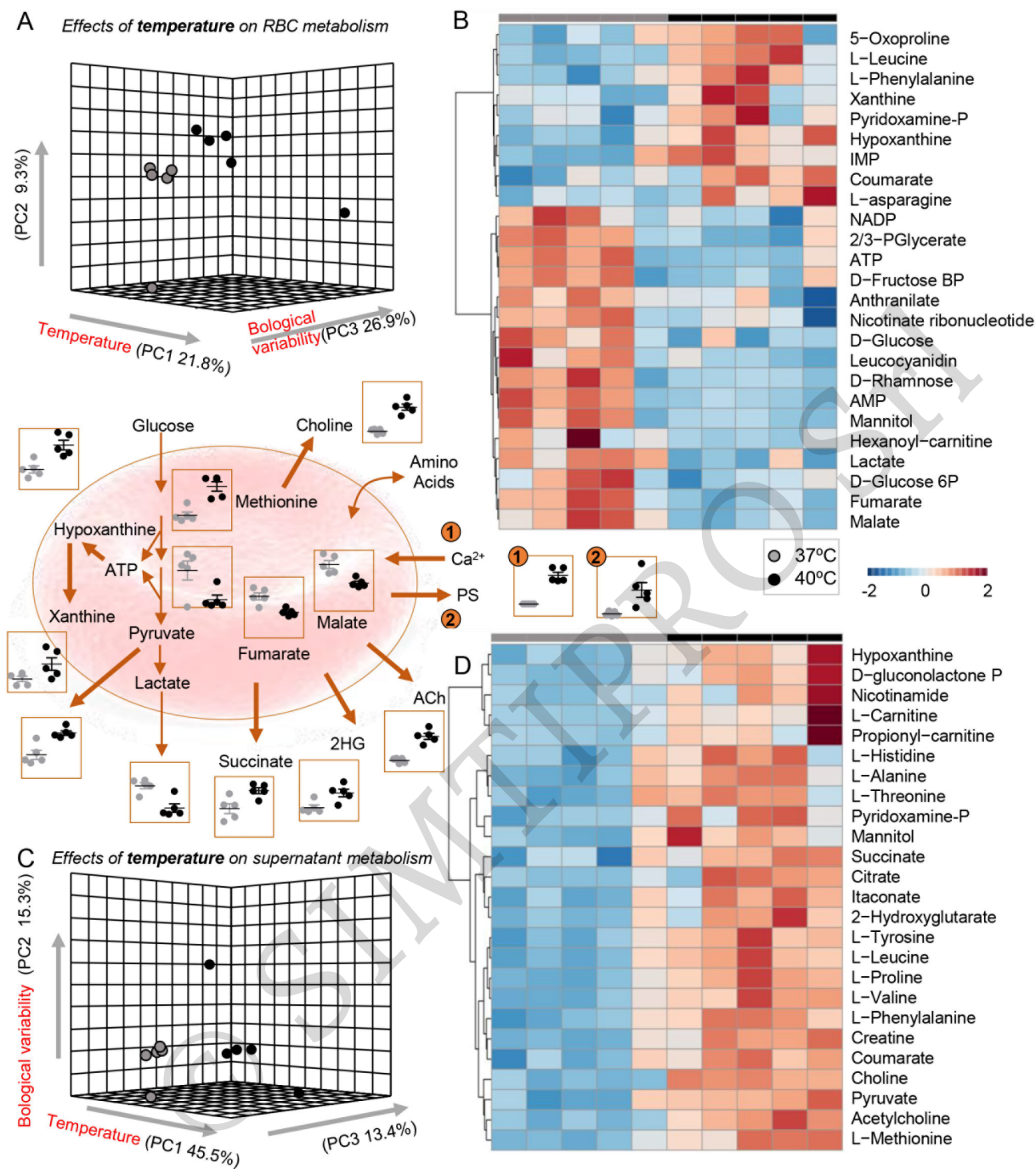


Figure 4 - Metabolic impact of hyperthermic stress.

(A and C) Partial least square-discriminant analyses (PLS-DA) reveals significant impact of high fever-like temperatures on RBCs and supernatants, respectively. (B and D) Top 25 significant metabolites following heat stress by ANOVA in RBCs and supernatants, respectively. Key metabolites are highlighted in the dot plots in the centre of the figure, colour-coded as per the legend on the right-hand side of the figure.

Ach: acetylcholine; ATP: adenosine triphosphate; 2HG: hydroxyglutarate.

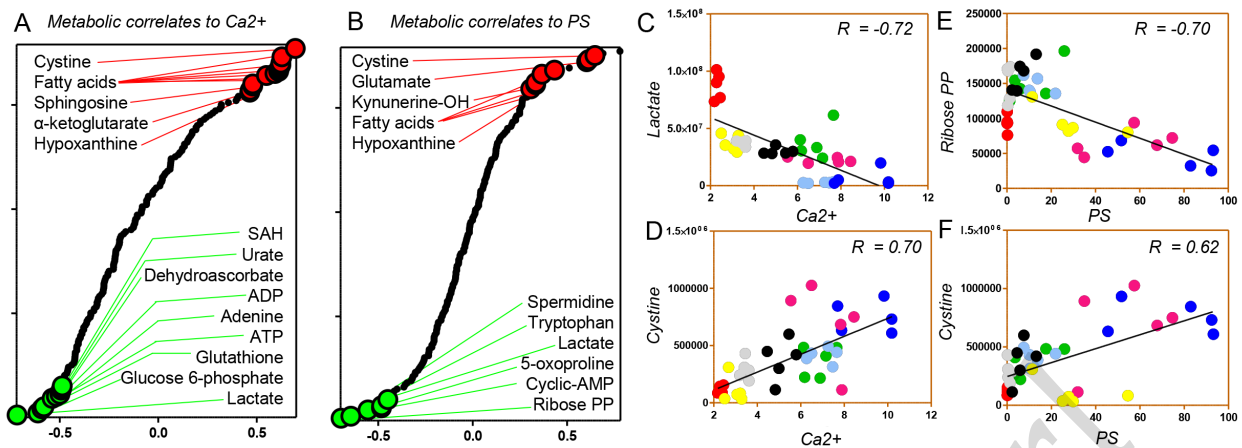


Figure 5 - Correlation analyses between red blood cell (RBC) death and metabolism.

Correlation analyses between metabolite measurements and intracellular Ca^{2+} level (A) or phosphatidylserine (PS) exposure (B). (C and D) Intracellular lactate or cystine levels are negative and positive correlates to intracellular Ca^{2+} levels, respectively. (E and F) Intracellular ribose-diphosphate or cystine levels are negative and positive correlates to PS exposure levels, respectively. (C-F) Stresses are colour-coded as in Figure 1.

ADP: adenosine diphosphate; ATP: adenosine triphosphate; SAH: S-adenosylhomocysteine.

breakdown (decreased ATP, increased IMP) and oxidation (hypoxanthine, xanthine), elevated markers of glutathione turnover (5-oxoproline) (Figure 4B). Heat stress also resulted in decreases in glycolysis and increases in pyruvate/lactate ratios (with higher levels of supernatant pyruvate), along with decreases in intracellular carboxylic acids and supernatant accumulation of hydroxyglutarate. Notably, choline and acetyl-choline increased in the supernatants of RBCs exposed to 40 °C (Figure 4D).

Correlation analyses between red blood cell death and metabolism

Metabolite levels were correlated to intracellular Ca^{2+} levels and PS exposure. In Figure 5A and B, significant positive (red) or negative (green) correlates are highlighted, along with highlights of lactate and ribose phosphate (Figure 5C and E) (negative correlates to intracellular Ca^{2+} and PS exposure, respectively) and cystine (positive correlates to both) (Figure 5D and F). Consistent with the considerations above, increases in free fatty acids, carboxylic acids (ketoglutarate), glutathione synthesis/turnover dysregulation (glutamate, cystine) and purine oxidation (hypoxanthine) was positively correlated to increases in intracellular Ca^{2+} and PS exposure, independently of the stress, consistent with increased cell death. *Vice versa*, negative correlates (suggestive of decreased apoptosis) were consistent with increases in high-energy phosphate compounds and total adenylate pools (ATP, ADP, adenine)

or purine signalling (cAMP), increases in glycolysis (lactate) and antioxidant metabolism (glutathione, urate, dehydroascorbate, SAM, glucose 6-phosphate and ribose phosphate as markers of PPP activation) (Figure 5).

DISCUSSION

The energy and redox state of a cell plays a critical role in regulating the cell's capacity to cope with stressors¹⁶. This holds true for nucleated cells, which can respond to stimuli by mechanism of regulation of gene expression to cope with sudden environmental changes. However, these considerations are even more relevant to the mature RBC, in which the lack of organelles and nuclei makes it impossible to cope with stressors through the synthesis of novel enzymes that could help in counteracting stressors such as heat or ionic stress through the synthesis of, for example, novel heat shock protein chaperones or ion transporters. Similarly, the lack of mitochondria deprives the RBC of the metabolic plasticity that characterises other cells with respect to the capacity to generate energy (in the form of nucleosides triphosphate) from sources other than glucose. Indeed, mitochondria are essential for the synthesis of ATP from fatty acid and amino acid catabolism. However, the advent of omics technologies has elucidated, over the past decade, the (unexpected) complexity of the RBC metabolome²⁵, paving the way for a significant expansion of our understanding of

the mechanisms that RBCs can leverage to cope with different stressors in order to avoid (or facilitate) cell death following environmental insults. Based on these considerations, in the present study we investigated the impact of starvation, ionic, hyperosmotic, and heat stress on RBC metabolism *via* UHPLC-MS-based metabolomics approaches. In recent years, we have extensively used this workflow to investigate the impact of refrigerated storage on RBC metabolism under all currently marketed storage additives^{12,14,23,26,27}. Results helped elucidate critical cross-talks between storage-induced depression of energy metabolism and the progressively irreversible alteration of RBC redox metabolism. Identified mechanisms involved donor-dependent²³ changes in the capacity to: (i) activate the PPP and generate reducing equivalent in the face of storage-induced oxidant stress^{15,28}; (ii) repair oxidatively damaged proteins^{29,30}. Despite critical differences between RBC ageing *in vivo* and *in vitro*³¹, we hypothesised that some of these mechanisms relevant to blood storage quality may be relevant to RBC physiology in the context of pathological stresses. For instance, refrigerated storage temperature are known to negatively impact RBC ion homeostasis, resulting in the intracellular accumulation of Ca²⁺ and the downstream activation of Ca²⁺-dependent proteases involved in RBC cell death³². Interestingly, here we noted that ionomycin-induced increases in intracellular Ca²⁺ levels resulted in metabolic aberrations comparable to those observed in stored RBCs, including decreased glycolysis³³, increased purine oxidation (consistent with activation of Ca²⁺-dependent RBC-specific AMP deaminase 3)³⁴, dysregulated carboxylic acid metabolism³⁴, and increased fatty acid mobilisation^{23,35,36}. On the other hand, we found that hypertonic stress due to incubation in higher concentrations of sucrose had opposite effects, resulting in the promotion of glycolysis, glutathione synthesis and a subtle intracellular Ca²⁺ accumulation. This observation may be critical for the formulation of novel blood storage additives with the goal to boost the aforementioned pathways²⁵, which tend to be inhibited progressively as a function of storage duration. Notably, glucose starvation in oxygen-rich environments results, in all eukaryotic cells in the human body but RBCs (i.e., in all cells that contain mitochondria), in a metabolic rewiring towards fatty acid catabolism. The first step in this pathway is constrained by the activation

of phospholipases to promote the release of fatty-acyl moieties from membrane lipids. Notably, RBCs are endowed with such enzymes, including non-canonical redox-sensitive phospholipases such as peroxiredoxin 6, an antioxidant enzyme that, in the face of (oxidant) stress, can migrate to the membrane and exert a phospholipase A₂-like activity³⁷. While some have shown that this activity can be Ca²⁺-independent³⁸, it is interesting to note that defects in energy metabolism can result in ATP depletion, which in turn impairs ATP-dependent ion pump capacity and promotes intracellular accumulation of Ca²⁺. Since a sub-group of phospholipase A₂s are Ca²⁺-sensitive, their activation would result in lipolysis and thus fuel mitochondria in cells with organelles, but not RBCs. Consistently, here we noted that glucose-starvation resulted in increases in free fatty acids, even when RBCs were incubated in Ca²⁺-free media. As such, it is apparent that the above-described cascade may represent an oversimplification of a much more complicated series of events potentially involving other molecular mediators. Clearly, preservation of phospholipid membrane symmetry is an ATP-dependent process mediated by flippase activity, which prevents the externalisation of PS and phosphatidylethanolamines as a function of stress. In the context of this study, we noted that PS externalisation is, indeed, mostly dependent on the dysregulation of Ca²⁺ homeostasis and it can be prevented when specific stressors (e.g., ATP-depleting glucose starvation) are coupled to the lack of Ca²⁺ in the media. In addition, another potential contributor to the cascades described above is AMP-activated protein kinase³⁹, a protein that senses imbalances in AMP/ATP ratios which plays a major role in RBC lifespan⁴⁰ and can be activated by Ca²⁺-mediated protein phosphatase A₂ activity⁴¹, an abundant protein in RBC at the cross-roads of redox sensing and membrane stability⁴². In this purview, it is worth noting that stresses inducing intracellular Ca²⁺ increases, like ionomycin and heat stress, not only were accompanied by decreases in ATP, but also resulted in increases in purine deamination and alterations of reactions associated with the homeostasis of reducing equivalents NADH and NADPH (i.e., pyruvate/lactate ratios³⁰, carboxylic acid metabolism³⁴, and the PPP). Consistent with a potential role of oxidant stress in RBC cell death cascades, it is worth noting that PPP activation

was only observed in starved RBCs in the absence of Ca^{2+} or RBCs exposed to hypertonic stress.

Activation of the PPP is known to be critical to RBC homeostasis, as RBCs from donors suffering from glucose 6-phosphate dehydrogenase (G6PD) deficiency (the most common enzymopathy in humans affecting approx. 400 million people) have a shorter lifespan⁴³. Compensatory mechanisms arise to cope with impaired antioxidant capacity in the G6PD-deficient RBCs, such as the over-activation of the NADH-dependent methemoglobin reductase³⁰. By depleting free NADH, methemoglobin reductase makes the last step of lactic fermentation downstream of glycolysis irrelevant, resulting in an accumulation of pyruvate and increased pyruvate/lactate ratios. Of note, glucose starvation (independently of Ca^{2+} depletion in the media) resulted in significant increases in pyruvate to lactate ratios.

From the untargeted analyses, several indole-containing tryptophan metabolites clustered with pyruvate and carboxylic acids. Notably, RBCs are endowed with five different transport systems, as identified by kinetic analyses and studies of inhibition and sodium dependence of transport: the L-, T-, Ly-, ASC- and Gly-system⁴⁴. Dysregulation of ion homeostasis was thus expected to impact amino acid uptake and release; a result confirmed by the present analysis. However, intracellular levels of glutamate and cysteine, precursors in the synthesis of glutathione, increased significantly only in the RBC exposed to glucose starvation in presence of Ca^{2+} in the media, suggestive of Ca^{2+} - (other than ATP-) dependency of glutathione synthesis in the mature RBC. Previous studies have noted that gamma-glutamyl-cysteine ligase (a rate-limiting enzyme in glutathione synthesis) is indeed activated *via* phosphorylation by protein kinase C or Ca^{2+} -dependent calmodulin kinase II⁴⁵.

Arginine and methionine metabolites, specifically polyamines such as spermidine, were observed to increase in the supernatants of stressed RBCs, especially as a result of heat stress and glucose starvation in Ca^{2+} -free media. While the role of arginine metabolism in the mature RBC is not completely understood, the presence of a functional arginase⁴⁶ and nitric oxide (NO) synthase⁴⁷ in the RBC suggests that polyamine synthesis in the stressed RBC could sacrifice NO synthesis capacity to promote the generation of these "primordial stress molecules" with

a strong (redox and osmolality) buffering capacity⁴⁸. Interestingly, polyamine synthesis intertwines recycling of purine catabolites, such as methylthioadenosine) and one-carbon metabolism through reactions that involve methionine and S-adenosylmethionine as precursors⁴⁹. Notably, mature RBCs use methionine-derived methyl-groups to repair damaged isoaspartyl moieties in proteins that are generated as a function of (oxidant) stress⁵⁰. Interestingly, this damage-repair pathway was up-regulated by all the tested stresses. In this context, it is interesting to note that membrane phospholipids can be alternative methyl-group donors, through pathways that promote the generation of choline from phosphatidylethanolamine and phosphatidylcholine lipid heads. The resulting excess in choline promotes the release of choline itself from the RBC; a phenomenon observed in the starved RBC and inhibited in ionomycin-treated RBCs. Interestingly, intracellular choline can be converted to acetylcholine, a metabolite that plays a key role in endothelial cell function, through reactions that are constrained by the availability of acetyl-CoA⁴⁶. In this study, different stressors impacted the levels of pantothenol, a precursor to CoA, as well as the levels of several fatty acyl-carnitines, which in the mature RBC are in equilibrium with free fatty acids, acyl-CoAs and carnitine levels, and are indicative of the status of homeostasis (or stress) of membrane lipids⁴⁶. Overall, these results are indicative of a potential role of RBC protein damage-repair mechanisms in choline metabolism.

CONCLUSION

In the present study, we investigated the metabolic impact of starvation, Ca^{2+} metabolism, extracellular hypertonicity, hyperthermia, and ionic stress in RBCs. As a result, we expand on existing literature highlighting the heterogeneity of RBC responses to different RBC cell death-inducing stressors. The results presented here can inform follow-up studies to mechanistically target specific metabolic pathways, with the goal of exacerbating or preventing RBC metabolic responses to pathological stresses. Since RBCs represent a simplified model of cellular ageing⁵¹, the present study sets the stage for future studies testing novel strategies to leverage metabolic control to improve RBC capacity to cope with stressors, and thus extend the lifespan of RBCs and other cells.

ACKNOWLEDGEMENTS

The Authors thank the Canadian Blood Services (CBS) Development Laboratory (netCAD) for providing processed blood components. The authors gratefully acknowledge the technical assistance of Varsha Bhakta at McMaster University. SMQ and WPS were supported by resources from CBS. WPS was funded by an intramural grant (IG2017-WS) from CBS. As a condition of Canadian government funding, this report must contain the statement, "The views expressed herein do not necessarily represent the view of the federal government of Canada."

AUTHORSHIP CONTRIBUTIONS

TN and SMQ are co-first authors.

TN performed the experiments, analysed the data, and prepared the figures. SMQ performed the experiments and contributed to study design and manuscript preparation. WPS contributed to the study design. ADA contributed to the study design and manuscript preparation.

CONFLICT OF INTERESTS

Though unrelated to the contents of the manuscript, the authors declare that AD and TN are founder of Omix Technologies Inc. and Altis Bioscience LLC. All the other authors have no conflicts of interest to disclose.

REFERENCES

1. Antonelou MH, Kriebardis AG, Papassideri IS. Aging and death signalling in mature red cells: from basic science to transfusion practice. *Blood Transfus* 2010; **8** (Suppl 3): s39-47.
2. Lutz HU, Bogdanova A. Mechanisms tagging senescent red blood cells for clearance in healthy humans. *Front Physiol* 2013; **4**: 387.
3. Lang E, Qadri SM, Lang F. Killing me softly - suicidal erythrocyte death. *Int J Biochem Cell Biol* 2012; **44**: 1236-43.
4. Qadri SM, Bissinger R, Solh Z, Oldenborg PA. Eryptosis in health and disease: a paradigm shift towards understanding the (patho) physiological implications of programmed cell death of erythrocytes. *Blood Rev* 2017; **31**: 349-61.
5. Pretorius E, du Plooy JN, Bester J. A comprehensive review on eryptosis. *Cell Physiol Biochem* 2016; **39**: 1977-2000.
6. Bissinger R, Bhuyan AAM, Qadri SM, Lang F. Oxidative stress, eryptosis and anemia: a pivotal mechanistic nexus in systemic diseases. *FEBS J* 2019; **286**: 826-54.
7. Arashiki N, Takakuwa Y, Mohandas N, et al. ATP11C is a major flippase in human erythrocytes and its defect causes congenital hemolytic anemia. *Haematologica* 2016; **101**: 559-65.
8. Ghashghaeinia M, Cluitmans JC, Akel A, et al. The impact of erythrocyte age on eryptosis. *Br J Haematol* 2012; **157**: 606-14.
9. Lang KS, Duranton C, Poehlmann H, et al. Cation channels trigger apoptotic death of erythrocytes. *Cell Death Differ* 2003; **10**: 249-56.
10. Gatto C, Milanick M. Red blood cell Na pump: insights from species differences. *Blood Cells Mol Dis* 2009; **42**: 192-200.
11. Yurkovich JT, Zielinski DC, Yang L, et al. Quantitative time-course metabolomics in human red blood cells reveal the temperature dependence of human metabolic networks. *J Biol Chem* 2017; **292**: 19556-64.
12. D'Alessandro A, Kriebardis AG, Rinalducci S, et al. An update on red blood cell storage lesions, as gleaned through biochemistry and omics technologies. *Transfusion* 2015; **55**: 205-19.
13. Reisz JA, Slaughter AL, Culp-Hill R, et al. Red blood cells in hemorrhagic shock: a critical role for glutaminolysis in fueling alanine transamination in rats. *Blood Adv* 2017; **1**: 1296-305.
14. Nemkov T, Sun K, Reisz JA, et al. Hypoxia modulates the purine salvage pathway and decreases red blood cell and supernatant levels of hypoxanthine during refrigerated storage. *Haematologica* 2018; **103**: 361-72.
15. Reisz JA, Wither MJ, Dzieciatkowska M, et al. Oxidative modifications of glyceraldehyde 3-phosphate dehydrogenase regulate metabolic reprogramming of stored red blood cells. *Blood* 2016; **128**: e32-42.
16. Mason EF, Rathmell JC. Cell metabolism: an essential link between cell growth and apoptosis. *Biochim Biophys Acta* 2011; **1813**: 645-54.
17. Halama A, Riesen N, Moller G, et al. Identification of biomarkers for apoptosis in cancer cell lines using metabolomics: tools for individualized medicine. *J Intern Med* 2013; **274**: 425-39.
18. Wu M, Ye H, Shao C, et al. Metabolomics-proteomics combined approach identifies differential metabolism-associated molecular events between senescence and apoptosis. *J Proteome Res* 2017; **16**: 2250-61.
19. van Wijk R, van Solinge WW. The energy-less red blood cell is lost: erythrocyte enzyme abnormalities of glycolysis. *Blood* 2005; **106**: 4034-42.
20. Arandjelovic S, Ravichandran KS. Phagocytosis of apoptotic cells in homeostasis. *Nat Immunol* 2015; **16**: 907-17.
21. Qadri SM, Chen D, Schubert P, et al. Pathogen inactivation by riboflavin and ultraviolet light illumination accelerates the red blood cell storage lesion and promotes eryptosis. *Transfusion* 2017; **57**: 661-73.
22. Nemkov T, Hansen KC, D'Alessandro A. A three-minute method for high-throughput quantitative metabolomics and quantitative tracing experiments of central carbon and nitrogen pathways. *Rapid Commun Mass Spectrom* 2017; **31**: 663-73.
23. D'Alessandro A, Culp-Hill R, Reisz JA, et al.; Recipient Epidemiology and Donor Evaluation Study-III (REDS-III). Heterogeneity of blood processing and storage additives in different centers impacts stored red blood cell metabolism as much as storage time: lessons from REDS-III-Omics. *Transfusion* 2019; **59**: 89-100.

24. Clasquin MF, Melamud E, Rabinowitz JD. LC-MS data processing with MAVEN: a metabolomic analysis and visualization engine. *Curr Protoc Bioinformatics* 2012; **37**: 14.11.1-14.11.23.
25. Nemkov T, Reisz JA, Xia Y, et al. Red blood cells as an organ? How deep omics characterization of the most abundant cell in the human body highlights other systemic metabolic functions beyond oxygen transport. *Expert Rev Proteomics* 2018; **15**: 855-64.
26. Gehrke S, Srinivasan AJ, Culp-Hill R, et al. Metabolomics evaluation of early-storage red blood cell rejuvenation at 4 degrees C and 37 degrees C. *Transfusion* 2018; **58**:1980-91.
27. D'Alessandro A, Gray AD, Szczepiorkowski ZM, et al. Red blood cell metabolic responses to refrigerated storage, rejuvenation, and frozen storage. *Transfusion* 2017; **57**: 1019-30.
28. Wither M, Dzieciatkowska M, Nemkov T, et al. Hemoglobin oxidation at functional amino acid residues during routine storage of red blood cells. *Transfusion* 2016; **56**: 421-6.
29. Kriebardis AG, Antonelou MH, Stamoulis KE, et al. Progressive oxidation of cytoskeletal proteins and accumulation of denatured hemoglobin in stored red cells. *J Cell Mol Med* 2007; **11**: 148-55.
30. Tzounakas VL, Kriebardis AG, Georgatzakou HT, et al. Glucose 6-phosphate dehydrogenase deficient subjects may be better "storers" than donors of red blood cells. *Free Radic Biol Med* 2016; **96**: 152-65.
31. Bosman GJ, Werre JM, Willekens FL, Novotny VM. Erythrocyte ageing in vivo and in vitro: structural aspects and implications for transfusion. *Transfus Med* 2008; **18**: 335-47.
32. Koshkaryev A, Zelig O, Manny N, et al. Rejuvenation treatment of stored red blood cells reverses storage-induced adhesion to vascular endothelial cells. *Transfusion* 2009; **49**: 2136-43.
33. Gevi F, D'Alessandro A, Rinalducci S, Zolla L. Alterations of red blood cell metabolome during cold liquid storage of erythrocyte concentrates in CPD-SAGM. *J Proteomics* 2012; **76** (Spec No.): 168-80.
34. Nemkov T, Sun K, Reisz JA, et al. Metabolism of citrate and other carboxylic acids in erythrocytes as a function of oxygen saturation and refrigerated storage. *Front Med (Lausanne)* 2017; **4**: 175.
35. de Wolski K, Fu X, Dumont LJ, et al. Metabolic pathways that correlate with post-transfusion circulation of stored murine red blood cells. *Haematologica* 2016; **101**: 578-86.
36. Fu X, Felcyn JR, Odem-Davis K, Zimring JC. Bioactive lipids accumulate in stored red blood cells despite leukoreduction: a targeted metabolomics study. *Transfusion* 2016; **56**: 2560-70.
37. Fisher AB. Peroxiredoxin 6: a bifunctional enzyme with glutathione peroxidase and phospholipase A(2) activities. *Antioxid Redox Signal* 2011; **15**: 831-44.
38. Moawad AR, Fernandez MC, Scarlata E, et al. Deficiency of peroxiredoxin 6 or inhibition of its phospholipase A2 activity impair the in vitro sperm fertilizing competence in mice. *Sci Rep* 2017; **7**: 12994.
39. Zelenak C, Foller M, Velic A, et al. Proteome analysis of erythrocytes lacking AMP-activated protein kinase reveals a role of PAK2 kinase in eryptosis. *J Proteome Res* 2011; **10**: 1690-7.
40. Foller M, Sopjani M, Koka S, et al. Regulation of erythrocyte survival by AMP-activated protein kinase. *FASEB J* 2009; **23**: 1072-80.
41. Park S, Scheffler TL, Rossie SS, Gerrard DE. AMPK activity is regulated by calcium-mediated protein phosphatase 2A activity. *Cell Calcium* 2013; **53**: 217-23.
42. Pantaleo A, Ferru E, Pau MC, et al. Band 3 erythrocyte membrane protein acts as redox stress sensor leading to its phosphorylation by p (72) syk. *Oxid Med Cell Longev* 2016; **2016**: 6051093.
43. Arese P, Gallo V, Pantaleo A, Turrini F. Life and death of glucose-6-phosphate dehydrogenase (G6PD) deficient erythrocytes - role of redox stress and band 3 modifications. *Transfus Med Hemother* 2012; **39**: 328-34.
44. Rosenberg R. Amino acid transport in human red blood cells. *Acta Psychiatr Scand Suppl* 1988; **345**: 25-8.
45. Sun WM, Huang ZZ, Lu SC. Regulation of gamma-glutamylcysteine synthetase by protein phosphorylation. *Biochem J* 1996; **320**: 321-8.
46. D'Alessandro A, Reisz JA, Zhang Y, et al. Effects of aged stored autologous red blood cells on human plasma metabolome. *Blood Adv* 2019; **3**: 884-96.
47. Kleinbongard P, Schulz R, Rassaf T, et al. Red blood cells express a functional endothelial nitric oxide synthase. *Blood* 2006; **107**: 2943-51.
48. Rhee HJ, Kim EJ, Lee JK. Physiological polyamines: simple primordial stress molecules. *J Cell Mol Med* 2007; **11**: 685-703.
49. Paglia G, D'Alessandro A, Rolfsson O, et al. Biomarkers defining the metabolic age of red blood cells during cold storage. *Blood* 2016; **128**: e43-50.
50. Barber JR, Clarke S. Membrane protein carboxyl methylation increases with human erythrocyte age. Evidence for an increase in the number of methylatable sites. *J Biol Chem* 1983; **258**: 1189-96.
51. Kaestner L, Minetti G. The potential of erythrocytes as cellular aging models. *Cell Death Differ* 2017; **24**: 1475-7.